Polymer 50 (2009) 5427–5433

Contents lists available at ScienceDirect

Polymer

journal homepage: www.elsevier.com/locate/polymer

Synthesis and characterization of stereotriblock polybutadiene containing crystallizable high *trans*-1,4-polybutadiene block by barium salt of di(ethylene glycol) ethylether/triisobutylaluminium/dilithium

Xuetao Zhang, Yang Li*, Chunqing Zhang, Yanming Hu, Shunxi Song, Huanhuan Guo, Yurong Wang

State Key Laboratory of Fine Chemicals, Department of Polymer Science and Engineering, Dalian University of Technology, Dalian, 116012, China

ARTICLE INFO

Article history:
Received 8 May 2009
Received in revised form
24 September 2009
Accepted 25 September 2009
Available online 1 October 2009

Keywords:
Stereotriblock polybutadiene
Cold crystallization
Anionic polymerization

ABSTRACT

A series of high *trans*-1,4-low-*cis*-1,4-high *trans*-1,4-stereotriblock polybutadienes (HTPB-*b*-LCPB-*b*-HTPBs) were synthesized through a sequential anionic polymerization of butadiene (Bd) initiated by barium salt of di(ethylene glycol) ethylether/triisobutylaluminium/dilithium (BaDEGEE/TIBA/DLi). The polymers consisted of elastic low-*cis*-1,4-polybutadiene (LCPB) chemically bonded with crystallizable high *trans*-1,4-polybutadiene (HTPB). The block ratios (HTPB:LCPB:HTPB) were designed at 25:50:25 (molar ratio) and finally determined by SEC. The microstructures and sequences of the specimens were investigated by FTIR and NMR. The resultant HTPB-*b*-LCPB-*b*-HTPBs consisted of LCPB block with 52.5% *trans*-1,4 content and HTPB block with 55.9–85.8% *trans*-1,4 content. According to differential scanning calorimetry (DSC), HTPB-*b*-LCPB-*b*-HTPB showed a significant cold crystallization which was discussed in terms of entanglement concept. The cold crystallization temperature (T_{cc}) decreased whereas the melting temperature (T_m) increased with the increasing *trans*-1,4 content of HTPB block.

1. Introduction

Stereo block polybutadiene often exhibits micro-phase separation transition and allows the new complex morphologies due to the balance of relative incompatibility and molecular architectures with unique qualities, which the classical polymer blend cannot show [1–4]. However, up to now, only a few kinds of stereotriblock polybutadiene have been reported. By means of anionic polymerization, 1,2-1,4-1,2-stereotriblock polybutadiene was prepared by Wang [3] and Xie [4], respectively. The polymer had two T_gs and two loss moduli and exhibited micro-phase separation. Further more, 1,2-1,4-1,2-stereotriblock polybutadiene was hydrogenated to be (butene-1-ethylene-butene-1) tri-block copolymer which consisted of more than 30% crystallinity and exhibited the behavior of a thermoplastic elastomer [4].

Consequently, it is significant to synthesize stereotriblock polybutadiene containing crystallizable high *trans*-1,4-polybutadiene (HTPB) block due to the excellent mechanical properties of HTPB, including excellent antifatigue, low rolling resistance, low heat buildup, good green strength and low abrasion loss, which are necessary for the manufacture of products such as high performance tires [5–7].

It has been demonstrated that HTPB can be obtained by titanium [8,9], vanadium [10], and neodymium [11] catalyst systems. The *trans*-1,4 content of HTPB obtained by these catalyst systems is more than 90%, and great crystalline tendency is observed. However, these methods are inferior to anionic polymerization for synthesizing block copolymers, since they produce significant amount of homopolymers.

Potassium-based anionic initiation system can prepare HTPB with 80–95% of *trans*-1,4 content and has acceptable activity. However, they do not hold a "living" character, and the polymer is a heterogeneous mixture due to a number of insoluble HTPB [12,13]. Furthermore, a new anionic initiation system had been reported to obtain HTPB [14–19]. This initiation system showed good solubility in non-polar hydrocarbon solvents (such as cyclohexane), as well as reproducibility, commercial availability, and "living" character. However, to our knowledge, there is no report on the preparation of stereotriblock polybutadiene containing HTPB block.

The aim of the present article is to synthesize stereotriblock polybutadiene containing HTPB block. In this study, the preparation and characterization of high *trans*-1,4-low-*cis*-1,4-high *trans*-1,4-stereotriblock polybutadiene (HTPB-*b*- LCPB-*b*-HTPB) using barium salt of di(ethyleneglycol) ethylether (BaDEGEE)/triisobutylaluminum

* Corresponding author. Tel.: +86 0411 39893856; fax: +86 0411 83633080.
E-mail address: liyang@dlut.edu.cn (Y. Li).

0032-3861/$ – see front matter © 2009 Elsevier Ltd. All rights reserved.
doi:10.1016/j.polymer.2009.09.070

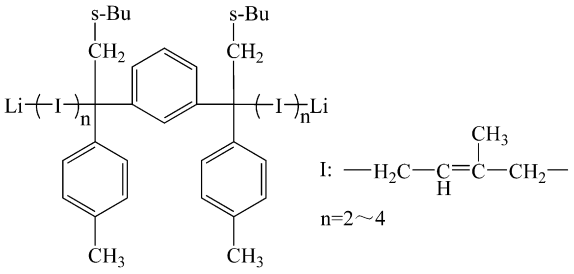

Chart 1. Structure of DLi.

(TIBA)/dilithium (DLi) as initiation system were described. The polymers had well controlled microstructures and macromolecular architecture determined by FTIR, NMR, and SEC. The thermal behaviors were recorded by differential scanning calorimetry (DSC), and the cold crystallization and melting were discussed in detail.

2. Experimental section

2.1. Materials

1,3-Butadiene (Bd, polymerization grade, Beijing Yanshan Petrochemical Co., China) was purified with a small amount of *sec*-butyllithium (*s*-BuLi) and then vaporized to keep water content below 10 ppm. *s*-BuLi (1.3 M solution in cyclohexane/hexane (92/8), Acros Organics Co., Geel, Belgium) and triisobutylaluminium (TIBA, 1.1 M solution in toluene, Acros Organics Co., Geel, Belgium) were diluted in dry cyclohexane under dry nitrogen, respectively. The concentration of *s*-BuLi was calibrated by Gilman double titration method [20]. The concentration of TIBA was calibrated by EDTA complexation titration method [21]. Cyclohexane (analytical reagent, Liaoyang Petrochemical Co., China) was dried and kept over molecular sieves (5Å) to keep water content below 5 ppm, and then it was purged with highly purified nitrogen for more than 15 min prior use to keep oxygen content below 10 ppm.

Barium di(ethylene glycol) ethyl ether (BaDEGEE) was synthesized according to the literature procedure [19].

2.2. The synthesis of dilithium

The synthesis of dilithium was described in the literatures [22,23]. Further more, several isoprene (Ip) units were added to

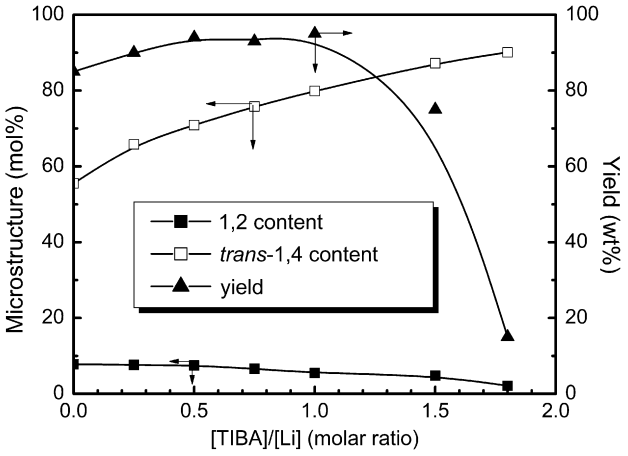

Fig. 1. Effects of [TIBA]/[Li] on microstructures and yield ([BaDEGEE]/[Li] = 0.25, [DLi]/Bd = 1.0 mmol/100 g, 70 °C).

C^-Li^+ bond to enhance the solubility of the dilithium in cyclohexane. The dilithium we adopted in the polymerization was simplified as DLi (Chart 1). The concentration of DLi was approximately 0.06 mol/L determined by the double titration method of Gilman [20].

2.3. Synthesis of HTPB-b-LCPB-b-HTPB

The synthesis of HTPB-*b*-LCPB-*b*-HTPB (simplified as HLH) was presented in Scheme 1. The LCPB block was prepared with Bd (30.0 g, 10 wt% in cyclohexane) initiated by DLi (0.3 mmol, 0.06 mol/L in cyclohexane) at 70 °C, which results in approximately 52.5% *trans*-1,4 units, 39.7% *cis*-1,4 units, and 7.8% 1,2 units. After completion of the polymerization, the temperature was lowered to 20 ± 1 °C and 6.0 g of the living polymer was terminated by degassed isopropanol for further analysis. The remaining living polymer was divided into six approximately equal parts, and each part was added into a stoichiometric amount of BaDEGEE ([BaDEGEE]/[Li] = 0.25) and TIBA ([TIBA]/[Li] = 0–1.5), which have been shown to produce high *trans*-1,4 addition under the conditions employed. Then quantitive Bd (equals to the remaining living polymer in the reactor) in cyclohexane, which had been purified by *s*-BuLi, was introduced into the reactor. The polymerization proceeded for another 3 h at 70 °C. After finishing the polymerization,

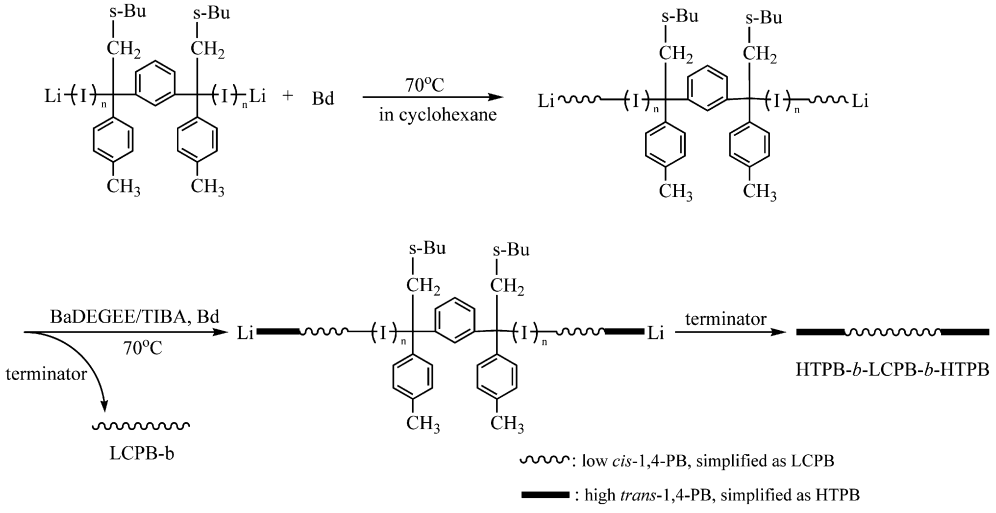

Scheme 1. Schematic presentation for the synthesis of HTPB-*b*-LCPB-*b*-HTPB.

Table 1
Characteristics of HTPB-*b*-LCPB-*b*-HTPBs and corresponding homopolybutadienes.

Sample	[TIBA]/[Li][a]	Microstructure[b] (mol%)			M_n[c]/10^4 (g/mol)	M_w/M_n[c]	Iv[c] (dl/g)	R_h[c] (nm)	φ_{HTPB}[d]
		trans-1,4	1,2-	*cis*-1,4					
LCPB-b	0.00[e]	52.5	8.0	39.5	5.46	1.06	0.7557	8.807	–
HLH-1	0.00	54.0 (55.9[f])	7.9	36.8	9.84	1.38	1.2265	13.426	0.45
HLH-2	0.25	59.2 (66.1[f])	7.8	31.1	10.68	1.13	1.2203	13.087	0.49
HLH-3	0.50	61.7 (69.3[f])	7.8	29.5	12.03	1.25	1.4732	14.909	0.55
HLH-4	0.75	64.2 (74.1[f])	6.6	27.3	11.85	1.18	1.5655	14.903	0.54
HLH-5	1.00	67.2 (78.5[f])	6.6	24.2	12.56	1.34	1.7385	16.125	0.57
HLH-6	1.50	70.9 (85.8[f])	5.5	21.6	12.21	1.48	1.8163	16.971	0.55
HTPB-c	0.50	71.0	6.6	22.4	6.18	1.31	0.8507	10.132	–
HTPB-b	1.50	87.2	4.8	8.0	6.89	1.19	1.0785	11.059	–

[a] [BaDEGEE]/Bd = 0.5 mmol/100 g.
[b] Determined by ^{13}C NMR and calculated according to ref. 26 and ref. 27.
[c] Measured by SEC in THF at 30 °C, referred to polystyrene standards.
[d] The fraction of HTPB block in HTPB-*b*-LCPB-*b*-HTPB, calculated according to equation (1).
[e] Without adding BaDEGEE.
[f] The *trans*-1,4 content of HTPB block (t_2) in HTPB-*b*-LCPB-*b*-HTPB, calculated according to equation (2).

the triblock polymer was terminated by a small amount of degassed isopropanol containing 2.5% w/v 2,6,4-antioxidant, precipitated by the addition of an excess amount of neat ethanol, and then dried in a vacuum oven at 40 °C. To be used as reference, a series of homopolybutadienes with 55–90% *trans*-1,4 content were synthesized by the similar procedure above except that BaDEGEE and TIBA were added along with DLi.

2.4. Characterizations

Infrared (IR) spectra of the polymers were recorded on a Nicolet FTIR spectrophotometer (USA) with films on NaCl discs.

^1H NMR and ^{13}C NMR were recorded on a 400 MHz Varian INOVA NMR (USA) spectrometer, with the tetramethylsilane as an internal reference.

Differential scanning calorimetry (DSC) measurements were conducted with a NETZSCH DSC 204 instrument (Germany). The calorimeter was calibrated with indium standard. About 8–10 mg samples were used at a heating rate of 10 °C/min under a flow of nitrogen (20 ml/min).

SEC experiments in THF were carried out at 30 °C with a Viscotek TDA302 instrument (USA) equipped with tetra detectors (RI, UV, LALS/RALS, and Viscometer). The concentration of the injected solution sample was approximate 2 mg/ml in all cases and the flow rate was 1 ml/min.

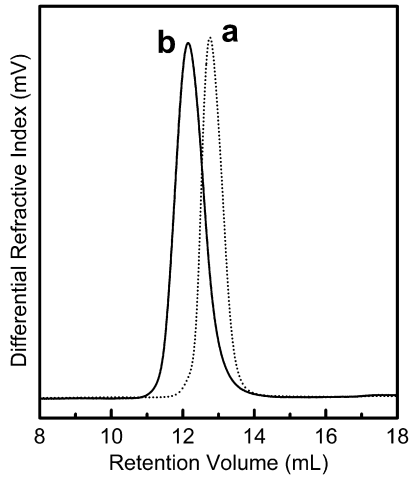

Fig. 2. SEC chromatograms in THF for the synthesis of HTPB-*b*-LCPB-*b*-HTPB: (a) LCPB-b ($M_n = 5.46 \times 10^4$, $M_w/M_n = 1.06$); (b) HTPB-*b*-LCPB-*b*-HTPB ($M_n = 12.03 \times 10^4$, $M_w/M_n = 1.25$).

3. Results and discussion

3.1. The macromolecular architecture design

In order to control the *trans*-selectivity of polybutadiene, BaDEGEE and TIBA were selected to complex with DLi to form the initiation system. The effects of [TIBA]/[Li] (molar ratio) on the microstructures were investigated, meanwhile keeping constant [BaDEGEE]/[Li] (molar ratio, 0.25/1.00). As shown in Fig. 1, the *trans*-1,4 content increases from 55.5% to 90.1% with the increasing of [TIBA]/[Li] from 0.0 to 1.8, while the 1,2 content decreases from 7.8% to 3.1%. Meanwhile, the yield increases slightly and then decreases sharply when [TIBA]/[Li] is higher than 1.0. Furthermore, it is unable to polymerize Bd when [TIBA]/[Li] is higher than 2.0 under the experimental conditions investigated (i.e., 70 °C for 3 h).

This interesting phenomenon is due to the "retarding effects" in the presence of TIBA [24]. High TIBA concentration in the composition of the initiator system transforms the living chain into inactive complexes, which can be explained by the formation of $LiAlR_4$ complex known to be inactive in the polymerization of Bd [25]. In other words, [TIBA]/[Li] is a key factor to synthesize HTPB-*b*-LCPB-*b*-HTPB containing crystallizable HTPB block with different *trans*-1,4 contents. By adjusting [TIBA]/[Li], a series of HTPB-*b*-LCPB-*b*-HTPBs containing crystallizable HTPB block were prepared. The microstructures of HTPB-*b*-LCPB-*b*-HTPBs determined by ^{13}C NMR spectra [26,27] are listed in Table 1.

Fig. 2 shows the SEC chromatograms of LCPB-b and HTPB-*b*-LCPB-*b*-HTPB (HLH-3, Table 1). From Fig. 2, we can conclude that

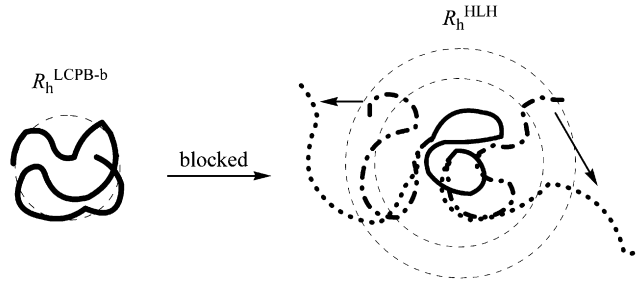

Fig. 3. The R_hs of LCPB block and HTPB-*b*-LCPB-*b*-HTPB with lower t_2 (dash dot line) and higher t_2 (dot line).

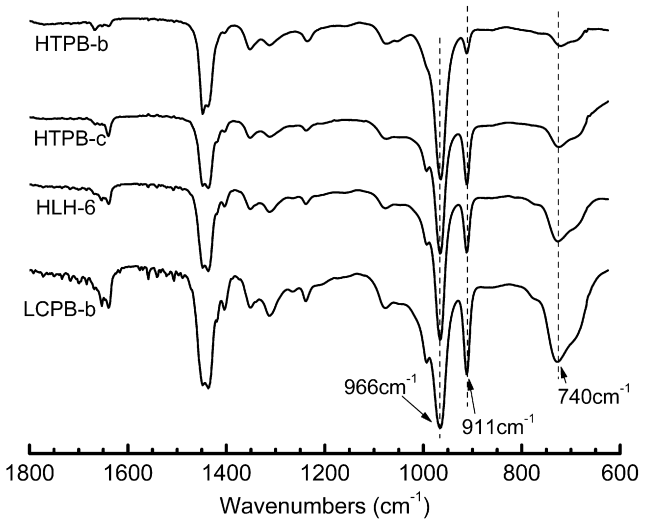

Fig. 4. The FTIR spectra of HLH-6 and corresponding homopolybutadienes.

well-defined tri-block copolymers were obtained. The fraction of HTPB block (Φ_{HTPB}) is calculated based on the following equation:

$$\Phi_{HTPB} = \frac{M_n^{HLH} - M_n^{LCPB}}{M_n^{HLH}} \quad (1)$$

where M_n^{LCPB}, M_n^{HLH} are the number average molecular weights of LCPB block and HTPB-*b*-LCPB-*b*-HTPB, respectively. Further more, the *trans*-1,4 content of HTPB block (t_2) is equal to:

$$t_2 = \frac{t - (1 - \Phi_{HTPB}) \times t_1}{\Phi_{HTPB}} \quad (2)$$

where t_1, t are the *trans*-1,4 content of LCPB block and HTPB-*b*-LCPB-*b*-HTPB, respectively. The results are presented in Table 1. As shown in Table 1, t_2 increases from 55.9% to 85.8%, which indicates that $LCPB^-Li^+$-$LCPB^-Li^+$ along with BaDEGEE and TIBA is capable of reinitiating the polymerization of Bd to obtain HTPB block. It is significant that this kind of tri-block PB is unique since it contains, for the first time, HTPB block with different *trans*-1,4 contents in a series of decreasing flexibility.

3.2. The molecular size

The detail molecular characteristics of the tri-block polymers are shown in Table 1. After been blocked, the molecular weight distribution (M_w/M_n) becomes broader. This phenomenon is attributed to the formation of the initiator complex, which results in slowing the initiation rate. The hydrodynamic radius (R_h) of HTPB-*b*-LCPB-*b*-HTPB is approximately twofold of that of LCPB block, and the same result is found in intrinsic viscosity (I_v). This observation can be explained by the longer chain length as shown in Fig. 3. It is interesting to notice that although the chain lengths of HTPB-*b*-LCPB-*b*-HTPBs are approximately the same, R_h increases from 13 nm to 17 nm along with the increasing t_2. This is attributed to the decreasing flexibility which reduces the chain entanglement and thus results in the increase of hydrodynamic volume (Fig. 3).

3.3. The microstructural difference between HTPB-b-LCPB-b-HTPB and homo-PB

To investigate the microstructural difference between HTPB-*b*-LCPB-*b*-HTPB and homo-PB, FTIR and NMR analysis are used. Take polymer HLH-6 for example, its first block is LCPB block (LCPB-b), and its second block is HTPB block (HTPB-b), and another HTPB (HTPB-c) containing similar *trans*-1,4 content to HLH-6 is selected for comparison. The FTIR spectra of LCPB-b, HLH-6, HTPB-c, and HTPB-b are shown in Fig. 4.

In the region between 600 and 1800 cm^{-1}, a number of vibrations of the three units are observed. The relative peak strength of

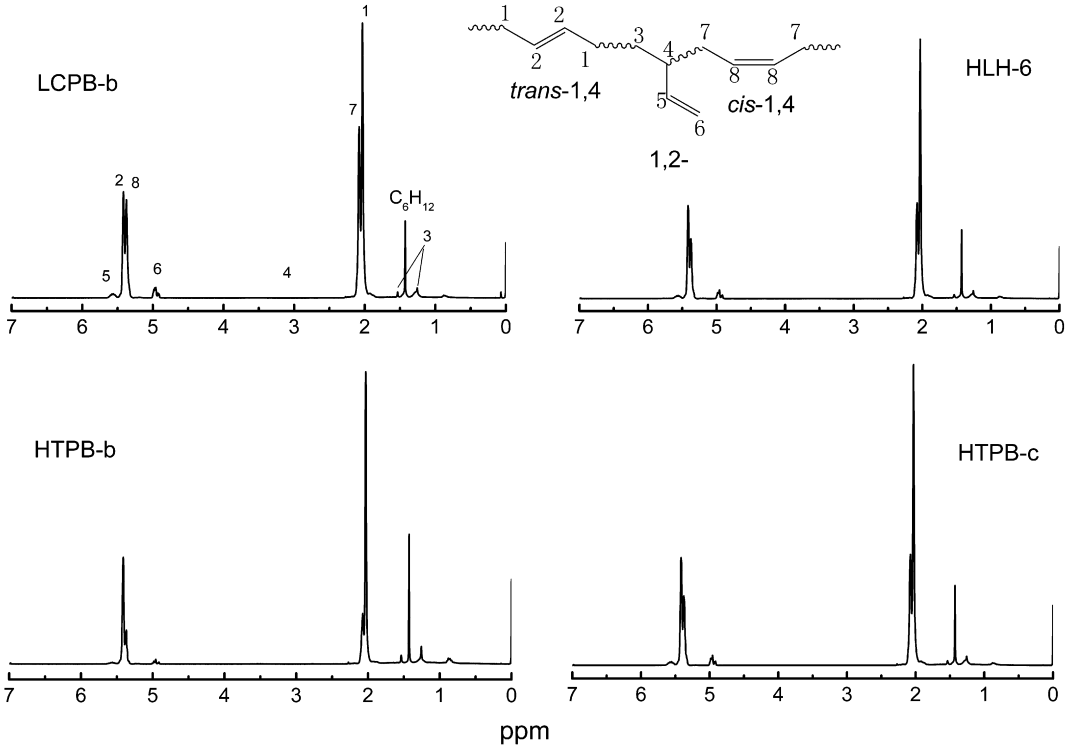

Fig. 5. The ^1H NMR spectra of HLH-6 and corresponding homopolybutadienes in $CDCl_3$ (C_6H_{12} is cyclohexane).

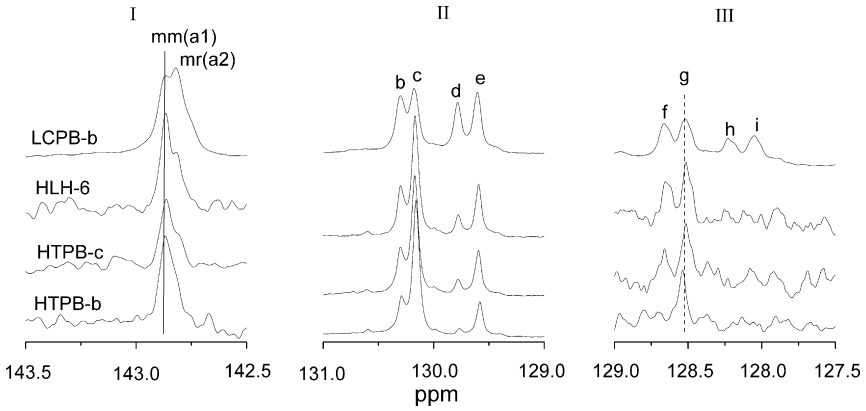

Fig. 6. Expanded ^{13}C NMR spectra of HLH-6 and corresponding homopolybutadienes in $CDCl_3$.

bands at 740 cm^{-1}, which represents the *cis*-1,4 units, decreases in the order: LCPB-b > HLH-6 ≈ HTPB-c > HTPB-b. In addition, the opposite result of bands at 966 cm^{-1} (represent the *trans*-1,4 units) is obtained.

Fig. 5 illustrates the ^1H NMR spectra of the samples with the assignment of all the protons. In all cases, weak peaks at 5.4 and 4.8 ppm, characteristic of 1,2 units, suggest main 1,4 addition product. It is difficult to determine the individual peak intensity of methane (signal 1 and 7) and vinyl (signal 2 and 8) protons of *trans*-1,4 units and *cis*-1,4 units because of the overlapping of those protons. However, it is clear that the peak intensity of the protons representing *cis*-1,4 units decreases in this order: LCPB-b > HLH-6 ≈ HTPB-c > HTPB-b. This result agrees well with that obtained by FTIR.

To further investigate the detail microstructural difference between HLH and homo-PB, the expanded ^{13}C NMR spectra of the samples are shown in Fig. 6.

As shown in Fig. 6 (I), polymer LCPB-b and HLH-6 contain predominantly two adjacent signals at 142.86 ppm (a1) and 142.82 ppm (a2), which are assignable to tvt and tvc+vct sequences, respectively [26]. However, signal a2 is not evident in polymer HLH-6 and could not be observed in polymer HTPB-c and HTPB-b. Accordingly, it is hardly to form tvt, tvc or vct triads in the presence of BaDEGEE, TIBA, and DLi. Additionally, a1 and a2 have been assigned to vvv triads by Furukawa [28]. Because pairs of contiguous 1,2 units can have meso- or racemic- configurations, Furukawa have assigned a1 and a2 to mm and mr, respectively. Thus, the initiation system BaDEGEE-TIBA-DLi can hardly form mr configuration in Bd polymerization. The four major olefinic resonances observed for polymers are shown in Fig. 6 (II). The signals have been assigned on polymers with predominantly 1,4-structure to tc (signal b at 130.30 ppm), tt (signal c at 130.18 ppm), cc (signal d at 129.78 ppm), and ct (signal e at 129.60 ppm) diads in previous study [26]. The relative intensities of signal c at 130.18 ppm and signal d 129.78 ppm are directly proportional to relative amounts of *trans*-1,4 and *cis*-1,4 units in the polymers. The *cis*-1,4/*trans*-1,4 (molar ratio) decreases in the following order: LCPB-b > HLH-6 ≈ HTPB-c > HTPB-b. This observation suggests the same result obtained by FTIR and ^1H NMR. Fig. 6 (III) shows signal f, g, h, and i (128.66, 128.52, 128.23, and 128.05 ppm) which are attributed to vtc, vtt, vcc, and vct, in order of decreasing chemical shift. Signals h and i disappear in polymer HLH-6, HTPB-c and HTPB-b. This can refer to the impediment of vcc or vct triad formation by BaDEGEE-TIBA-DLi initiation system. When *trans*-1,4 content is high enough, signal g is hardly observed in polymer HTPB-b. It is due to the initiation system adopted in this study which introduces few 1,2 addition and minor *cis*-1,4 addition.

In all cases, the results obtained by FTIR, ^1H NMR, and ^{13}C NMR in this study indicates that the microstructures and sequences of

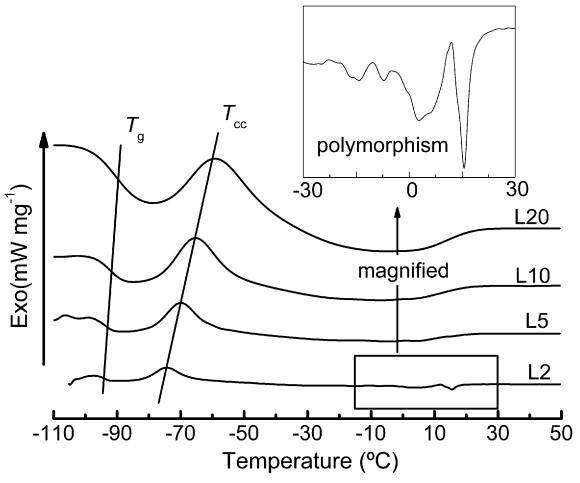

Fig. 7. DSC curves of HLH-6 at different programmed heating rate: (L2) 2 °C/min; (L5) 5 °C/min; (L10) 10 °C/min; (L20) 20 °C/min.

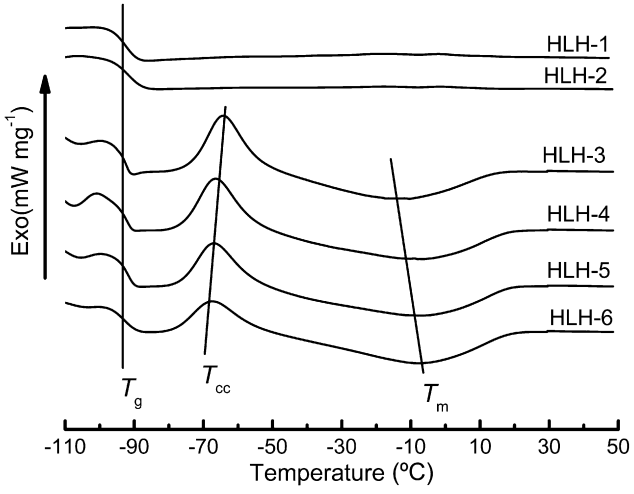

Fig. 8. DSC curves of HTPB-*b*-LCPB-*b*-HTPBs in the order of increasing *trans*-1,4 content.

Table 2
DSC data of HLH-6 obtained at different heating rates.

Run	R_H[a] (°C min^{-1})	T_g (°C)	T_{cc} (°C)	ΔC_p (J g^{-1} K^{-1})
L2	2	−94.0	−74.6	0.349
L5	5	−92.4	−70.0	0.466
L10	10	−90.9	−65.5	0.473
L20	20	−88.6	−59.4	0.482

[a] R_H means the heating rate.

tri-block polymer HLH are similar to those of HTPB-c and coincident with the mix of LCPB-b and HTPB-b.

3.4. Basic thermal behavior

The thermal property of HTPB-*b*-LCPB-*b*-HTPB was investigated by DSC analysis. The typical DSC curves (with different heating rate) of the sample (HLH-6) are shown in Fig. 7. An important variable in DSC measurement is the programmed heating rate (R_H). Increasing the heating rate improves the detectability of the transition. The position of the glass transition temperature (T_g) is shifted to high temperatures (Table 2). At the same time, the position of cold crystallization temperature (T_{cc}), which indicates the presence of the semi-crystalline HTPB domains, is shifted to high temperatures too. This variation of apparent T_g and T_{cc} with DSC heating rate has generally been attributed to the thermal lag of sample, which increases in step with the heating rate [29,30]. This thermal lag is considered to comprise a machine path error and a sample error which are dependent on the characteristics of the instrument and sample, respectively [31].

It is observed that the sample exhibits polymorphism during slow heating (magnified region of L2 in Fig. 7), because it shows two main endotherms (one is transition at 3 °C and the other one is fusion at 17 °C). This is due to the reorganization of the imperfect crystals [29]. Along with the increasing heating temperature, the imperfect crystals melt and that makes the chains around free to move, which introduces to retransform to high regularity crystal [32–35]. Before T_m, the melting of crystal with low regularity and the growing of the crystal with high regularity exist at the same time. The overlapping of the two thermal effects makes the melting process long [36]. Keeping on heating, the crystals both existed originally and transformed subsequently melt thoroughly.

Fig. 8 shows the DSC curves of HLH in the order of increasing t_2 with a heating rate of 10 °C min^{-1}. The six samples exhibit

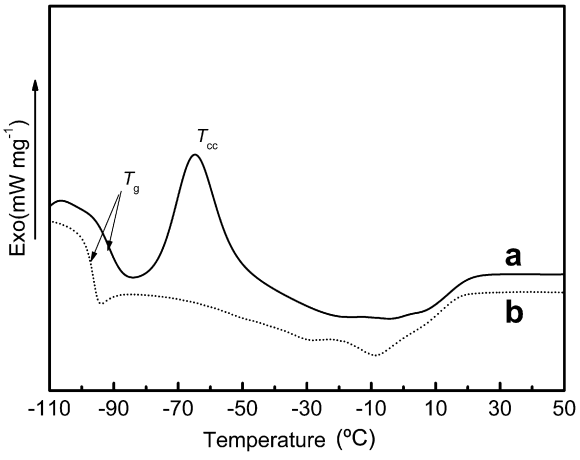

Fig. 9. DSC curves of HLH-6 obtained at different cooling rate: (a) 25 °C/min; (b) 2 °C/min. (Heating rate: 10 °C/min).

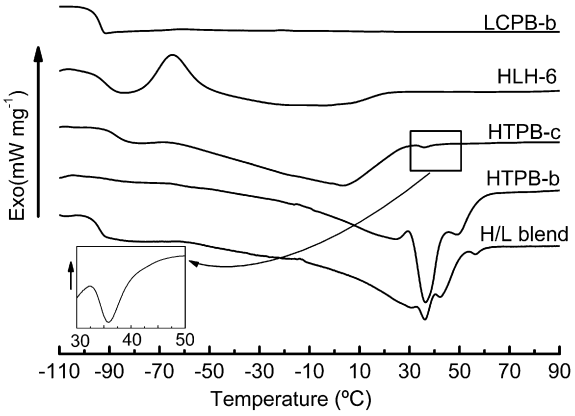

Fig. 10. DSC curves of HLH-6, corresponding homopolybutadienes and HTPB-b/LCPB-b blend (H/L blend, 50:50, by weight).

essentially the same T_g of approximately −92 °C. It is noteworthy that, in each sample of HLH-3 to HLH-6 ($t_2 > 70\%$), an exothermic peak (T_{cc}) corresponding to cold crystallization is observed above T_g and followed by a melting peak (T_m) below 0 °C. T_{cc} decreases whereas T_m increases with the increasing t_2, indicating that the cold crystallization happens readily in the sample with high t_2. In fact, the melting range of each sample containing cold crystallization peak is wide from about −50 to 20 °C. As we know, the tri-block copolymers might be thought that the morphology would consist of two phases each of which would have their own T_g [2,3]. However, only one T_g is observed. It is attributed to either the high level of HTPB crystallinity or the close T_g of HTPB and LCPB [37]. When the *trans*-1,4 content of HTPB block is low, the HTPB block is amorphous with one T_g near that of LCPB block; when the *trans*-1,4 content is high, the HTPB block is crystalline and exhibits one T_m; the others exhibit one T_g near that of LCPB and one T_m.

It has been reported that the high *cis*-1,4 PB (more than 95% *cis*-1,4 content) exhibits cold crystallization [38–40]. Crystallization of a polymer in its melt state involves transport and rearrangement of entangled chains in the vicinity of the crystal front [39]. The strong tendency of induced nucleation might be related to the strain of entangled chains at the crystal front in a manner similar to strain-induced crystallization of cross-linked rubber. Based on this, the cold crystallization peaks are introduced by the entanglement of semi-crystalline HTPB block and amorphous LCPB block. When the specimen is quickly quenched (10 °C min^{-1}, refers to Fig. 9a), there is not enough time for the crystallizable chain to reorganize. Then the sample exhibits rubbery and the frozen chain becomes free when being heated to above T_g, and semi-crystalline HTPB block domains becomes crystal because of being induced to reorganize into regular structure by amorphous LCPB block (see the evident exothermic peak in Fig. 9a). However, when the specimen is cooling slowly (2 °C min^{-1}, refers to Fig. 9b), the exothermic peak disappears and the melting becomes evident. This is attributed to the finishing reorganization of the semi-crystalline HTPB block during the slowly cooling.

3.5. The effect of HTPB block on the thermal behavior

It is well known that the *trans*-1,4 content has great effect on the thermal behavior of PB [17,33–35]. For example, HTPB with less than 65% of *trans*-1,4 content is amorphous, whereas HTPB with a number of *trans*-1,4 content greater than 80% is polymorphous and presents two endothermic transitions. The same result is obtained in LCPB-b and HTPB-b (Fig. 10). To investigate the effect of

HTPB block on the thermal behavior, LCPB-b and HTPB-b are blended with a ratio of 50:50 (referred to as H/L blend) for comparison. Another specimen (HTPB-c) whose microstructure is similar to HLH-6 is also selected, and the microstructural data are shown in Table 1. As shown in Fig. 10, LCPB-b exhibits amorphous with evident glass transition at −96 °C, while HTPB-b exhibits crystalline with obvious multi-melting between 30 and 50 °C, and the glass transition is ambiguous. The blended specimen (H/L blend) exhibits thermal feature both of LCPB-b and HTPB-b, and it is not significantly interactional between these two components. The thermal behavior changes greatly after being blocked (HLH-6) comparing with H/L blend. The feature of HLH-6 was discussed in detail hereinbefore. HTPB-c can be regarded as random distribution of LCPB-b and HTPB-b. It is evident to note that the cold crystallization disappears in HTPB-c, and the T_g shifts slightly to high temperature. Further more, HTPB-c has the tendency of multi-melting (magnified region in Fig. 10). In summary, the entanglement is strengthened by blocking HTPB-b and LCPB-b which results in the cold crystallization as discussed hereinbefore.

4. Conclusion

In summary, a series of HTPB-*b*-LCPB-*b*-HTPBs containing crystallizable HTPB block with 55.9–85.8% *trans*-1,4 content were prepared for the first time. The SEC analysis, which determined the block ratio as approximate 25:50:25, indicates that the R_h increases with the increasing *trans*-1,4 content of HTPB block. It is due to the decreasing flexibility of HTPB block. The results obtained by FTIR, ^{1}H NMR, and ^{13}C NMR in this study indicate that the microstructures and sequences of HLH-6 are similar to those of HTPB-c and coincident with the mix of LCPB-b and HTPB-b. It is noteworthy that the cold crystallization is observed when the *trans*-1,4 content of HTPB block is more than 70%, and when the specimen is cooling slowly, the cold crystallization disappears, which is due to the entanglement concept.

Acknowledgment

This work was financially supported by the National Nature Science Foundation of China (NNSFC 20674007 & 20774015) and China National Petroleum Corporation Innovation Fund (No. 05E7006).

References

[1] Halasa AF, Lohr DF, Hall JE. J Polym Sci 1981;19:1357.
[2] Bates FS, Bair HE, Hartney MA. Macromolecules 1984;17:1987.
[3] Wang YR, Li GH, Leng Y, Yang X, Gu MC. J Appl Polym Sci 2003;88:1049.
[4] Xie HQ, Ma LR. J Macromol Sci Pure Appl Chem 1985;22:1333.
[5] Hargis IG, Fabris HF, Living AR. US Patent, 1986; US 4616065.
[6] Harry SP, Hsu WL. US Patent, 1998; US 5844044.
[7] He AH, Huang BC, Huang YQ, Jiao SK. J. Appl. Polym. Sci. 2004;92:2941.
[8] Milione S, Cuomo C, Capacchione C, Zannoni C, Grassi A, Proto A. Macromolecules 2007;40:5638.
[9] Liguori D, Grisi F, Sessa I, Zambelli A. Macromol Chem Phys 2003;204:164.
[10] Monakov YB, Mullagaliev IR, Kharitonova EY. J Appl Polym Sci 2003;89:596.
[11] Urazbaev VN, Efimov VP, Sabirov ZM, Monakov YB. J Appl Polym Sci 2003;89:601.
[12] Halasa AF, Patterson DB. Macromolecules 1991;24:1583.
[13] Halasa AF, Patterson DB. Macromolecules 1991;24:4489.
[14] Hsu WL, Halasa AF. US Patent, 1992; US 5100965.
[15] Halasa AF, Hsu WL, Clites JS. US Patent, 2007; US 7285605.
[16] Halasa AF, Hsu WL, Jasiunas CA. US Patent, 2008; US 7321017.
[17] Benvenuta-Tapia JJ, Tenorio-Lopez JA, Herrera-Najera R, Rios-Guerrero L. Polym Eng Sci 2009;49:1.
[18] Benvenuta-Tapia JJ, Tenorio-Lopez JA, Herrera-Najera R. Macromol React Eng 2008;2:222.
[19] Zhang XT, Zhang CQ, Li Y, Guo HH, Song SX, Wang YR. Petrochemical Technology 2009;38:316.
[20] Gilman H, Haubein AH. J Am Chem Soc 1944;66:1515.
[21] Yuan LB, He R. Organic aluminum compounds. Bejing: People Press; 1979. p.127.
[22] Tung LH, Lo GYS. Macromolecules 1994;27:1680.
[23] Tung LH, Lo GYS. Macromolecules 1994;27:2219.
[24] Carlotti S, Menoret S, Barabanova A, Desbois P, Deffieux A. Polymer 2005;46:6836.
[25] Hsieh HL. J Polym Sci: Polym Chem Ed 1976;14:379.
[26] Wang HT, Bethea TW, Harwood HJ. Macromolecules 1993;26:715.
[27] van der Velden G, Didden C, Veermans T, Beulen J. Macromolecules 1987;20:1252.
[28] Furukawa J, Kobayashi E, Katsuki N, Kawagoe T. Die Makromolekulare Chemie 1974;175:237.
[29] Llers KH. Eur Polym J 1974;10:911.
[30] Burfield DR, Lim KL. Macromolecules 1983;16:1170.
[31] Strella S, Erhardt PF. J Appl Polym Sci 1969;13:1373.
[32] Hauser G, Schmidtke J, Strobl G. Macromolecules 1998;31:6250.
[33] Yang XN, Cai JL, Kong XH, Dong WM, Li G, Zhou EL. Macromol Chem Phys 2001;202:1166.
[34] Cai JL, Bo SQ, Li G, Zhou EL, Cheng RS. J Appl Polym Sci 2003;89:612.
[35] Wang PG, Woodward AE. Macromolecules 1987;20:2718.
[36] Zhu CS, Mo ZS, Xue XF, Wang JW. Polym Mater Sci Eng 1992;4:31.
[37] Switek KA, Chang K, Bates FS, Hillmyer MA. J Polym Sci Part A: Polym Chem 2007;45:361.
[38] Zhao H, Dong WM, Zhang XQ, Men YF. Chin J Appl Chem 2008;25:1233.
[39] Cheng TL, Su AC. Macromolecules 1993;26:7161.
[40] Su TK, Mark JE. Macromolecules 1977;10:120.